

Monte Carlo Simulation of Catalytic Reactions with Widely Varying Time Scales

L. V. LUTSEVICH¹ AND O. A. TKACHENKO

Computer Center of the Siberian Branch of the USSR Academy of Sciences, Pr. Acad. Lavrentjeva 6, Novosibirsk, 630090, USSR

Received October 2, 1991; revised January 14, 1992

An algorithm for Monte Carlo simulation (MC simulation) of catalytic reactions with widely varying time scales is described. The idea of the proposed algorithm is that the system is divided into "fast" and "slow" subsystems, which are simulated separately, each in its own time scale. A MC model of a heterogeneous catalytic reaction, $A + \frac{1}{2}B_2 \rightarrow AB$, which occurs through the Langmuir–Hinshelwood mechanism, supplemented with a slow stage of reversible adsorption of inert particles, is also investigated. It has been shown that, in this model, various relaxation oscillations exist and the rate constant of desorption of particles A is a crucial parameter in the formation of oscillations. © 1992 Academic Press, Inc.

In recent years, much attention has been focused on the study of the dynamic behavior of complicated chemical systems in which the rates of various processes are considerably different. For catalytic systems this may be associated with differences between fast processes of the main reaction and slow parallel processes, such as reversible oxidation of the catalyst surface, inert buffer adsorption, and changes in the gas phase (1–3). Models of such systems based on ordinary differential equations obtained assuming the surface to be uniform and employing the mass-action law are well studied (4–8). But in this field, the Monte Carlo method (MC method) is seldom used (9). The studies provided by MC models are well known to be of great interest because they allow one to investigate in detail the processes occurring on the surface and the effects caused by inhomogeneity of surface coverage. Study of complex dynamics (4–8) by MC models is also of great interest. However, there are certain difficulties associated

with this. MC simulation of the processes with sufficiently different time scales requires long computational time since in this case some probabilities are very small. In this paper a possible method of solving this problem is suggested.

It is useful to address well-known techniques used in qualitative analysis models of such systems, in particular the singular perturbation approach or its zeroth-order expansion, viz. the quasi-steady-state approximation (4, 10, 7). In both methods, the system is divided into two subsystems: one consists of slow processes and the other consists of fast ones. The "fast" subsystem is believed to be always in quasi-equilibrium state during all changes of the "slow" subsystem. This approach can be used in MC simulation of catalytic systems.

The idea of the proposed MC algorithm is that the system is divided into fast and slow subsystems and that they are then simulated separately, each in its own time scale. When the subsystems are simulated separately, it is possible to investigate the dynamics of the total system in the following sequence: (i) we change the state of the slow subsystem by a small quantity (ii) we restore the equilibrium state in the fast subsystem after ev-

¹ To whom correspondence should be addressed at Department of Chemical Engineering, The Pennsylvania State University, 133 Feuske Laboratory, University Park, PA 16802.

ery change in the slow one. It may turn out (this possibility is discussed later) that when a vast difference in the time scales of the subsystems exists, the number of events in the fast subsystem (per one event in the slow one) necessary to restore the equilibrium would be (in MC simulation) considerably less than the actual physical ratio. It is evident that for the total system not to deviate much from the steady state it is necessary that the slow subsystem change by small steps and the fast one reach the quasi-equilibrium state after every such step. Let us demonstrate with the following example.

Consider the reaction (its mechanism is not essential in this case) in which the origin of the coverage Θ_s is associated with the slow processes and that of the coverage Θ_f is associated with the fast ones. Let the slow processes be described by the set of the rate constants $\{K_i\}$, $i = 1, \dots, n$ and the fast ones by the set of $\{K_j\}$, $j = (n + 1), \dots, m$. The slow and the fast subsystems are then characterized by the time scales $\tau_s = 1/\Sigma K_i$ and $\tau_f = 1/\Sigma K_j$, respectively. Let us assume that $\tau_s \gg \tau_f$. To transform the rate constants into correspondent probabilities we multiply all constants K_i by time unit τ_s and all K_j by time unit τ_f :

$$P_i = K_i \tau_s, \quad P_j = K_j \tau_f.$$

In this case, probabilities P_i and P_j have maximum possible values $\Sigma P_i = 1$ and $\Sigma P_j = 1$. Note that since the probabilities for each subsystem are calculated separately, a proportional alteration of all rate constants in the slow subsystem does not influence the magnitudes of probabilities for either fast or slow subsystems. Such alteration results only in a change of t_s (time interval associated with the MC step). This means that the computational time does not depend on the real time scale of the slow processes. Assuming that the lattice consists of N sites, the surface coverages Θ_s and Θ_f are not equal to zero and coverage Θ_s is not in steady state.

1. First, we simulate the slow processes, choosing them at random in accordance

with P_i , then choosing at random the sites on the lattice, etc., in accordance with the mechanism of the slow processes. The time will be increased for each event by the increment

$$\Delta t = -(\tau_s \ln \xi)/N,$$

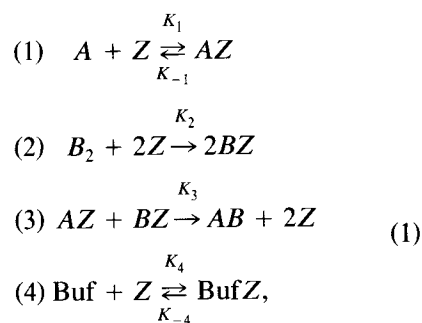
where $0 < \xi < 1$ is a pseudo-random number uniformly distributed on (0,1). We define the value of S_i , a step in changing the slow subsystem, as $S_i = \Delta \Theta_s / \Theta_s = 0.01$. The simulation continues until Θ_s changes by $\Delta \Theta_s = 0.01 \Theta_s$.

2. We simulate the fast processes only, choosing them at random in accordance with P_j , etc. The simulation continues until the fast subsystem reaches the quasi-equilibrium state. Then item 1 is carried out.

It is worthwhile to note that in simulating the fast processes (item 2) one need not measure their time, since the system changes in the time scale of slow processes.

VERIFICATION OF THE ALGORITHM

In this section, we verify the validity of the algorithm of time separate modeling (TSM). For this we compare the results obtained through TSM with those of the numerical solution of equations for the well-studied catalytic Langmuir-Hinshelwood reaction with the slow reversible adsorption of the inert buffer



where A , B_2 , and Buf are the particles in a gas phase and Z is an empty site on the surface of the catalyst. The model of this reaction employing the mass-action law (a mean field approximation, MFA) is

$$\begin{aligned}
\dot{\Theta}_A &= R_1 - R_{-1} - R_3, & \dot{\Theta}_Z &= R_{-1} - R_1 - R_2 - R_4 \\
\dot{\Theta}_B &= R_2 - R_3, & & + R_{-4} + 2R_3. \quad (2a) \\
\dot{\Theta}_{\text{Buf}} &= R_4 - R_{-4},
\end{aligned}$$

where R_i are the rates of the processes

$$\begin{aligned}
R_1 &= K_1\Theta_Z; & R_{-1} &= K_{-1}\Theta_A, & R_2 &= 2K_2\Theta_Z^2, \\
R_4 &= K_4\Theta_Z, & R_{-4} &= K_{-4}\Theta_{\text{Buf}}, \\
R_3 &= K_3\Theta_A\Theta_B,
\end{aligned}$$

and Θ_A , Θ_B , Θ_{Buf} , and Θ_Z are the coverages for AZ, BZ, BufZ, and Z, respectively, and K_i are the rate constants. The partial pressures P_A and P_{B_2} are included in K_1 and K_2 .

The MC model of mechanism (1) (without buffer stage 4) has been studied intensively (11–18). The case $K_3 \rightarrow \infty$, $K_{-1} = 0$, the well-known model ZGB (11), has been studied in detail. The MFA model of mechanism (1) has been studied in (5, 6, 19, 20) as well. It is established that in the MFA model, kinetic self-sustained oscillations occur which are caused by (i) differences in adsorption orders of the particles A and B₂, and (ii) the slow buffer stage (4). In (20), the set of rate constants ($K_1 = 0.85$, $K_{-1} = 0.3$, $K_2 = 1.23$, $K_4 = 0.001$, $K_{-4} = 0.0005$, $K_3 \cdot 10^3 - 10^5$) yields pronounced relaxation oscillations in the MFA model. However, the magnitudes of these constants cannot be used directly in the MC model to compare the results of MC modeling with those of the numerical integration in (20), because in the MFA model, the surface coverage is homogeneous while in the MC model it is inhomogeneous. The inhomogeneity of coverage influences considerably the kinetics of the two-site adsorption of B₂ and the reaction rate (and as a consequence, the total kinetics) so that the comparison itself makes no sense in this case (14, 18). One can try to obtain a homogeneous coverage in the MC model by allowing surface diffusion, but (at $K_3 \rightarrow \infty$) this requires a very long computational time. However, we can avoid these difficulties. We shall be able to deal directly with a MC model in which there is a homogeneous surface coverage if we solve Eqs. (2) by MC simulation. Equations (2) can be represented in the form of

To solve Eqs. (2a) with the MC technique, it is necessary to simulate directly the terms in its right side. In contrast to the inhomogeneous case, here one can directly simulate successful events if one calculates their probabilities through R_i values. This simulation must result in the behavior of the MC model for the case of homogeneous coverage. The general scheme of simulation of Eq. (2a) by the MC method at $K_3 \rightarrow \infty$ is given below. The above algorithm (TSM) is included in this scheme. The simulation is performed on the set of $N = 10,000$ ‘‘sites’’ and hence the coverage changes by $\Delta S = \pm 0.0001$ when one site becomes either occupied or vacated. Molecular act probabilities are calculated directly by the corresponding rates of processes as follows:

$$\begin{aligned}
P_4 &= R_4\tau_s \\
P_{-4} &= R_{-4}\tau_s \quad (3a)
\end{aligned}$$

$$\begin{aligned}
P_1 &= R_1\tau_f \\
P_{-1} &= R_{-1}\tau_f \quad (3b) \\
P_2 &= R_2\tau_f,
\end{aligned}$$

where $\tau_s = 1/(R_4 + R_{-4})$ and $\tau_f = 1/(R_1 + R_{-1} + R_2)$. Here, in compliance with the set of parameters (20), $R_{-2} = 0$. Pseudorandom numbers, ξ , uniformly distributed on (0,1) have been used for simulation.

1. First the slow subsystem is simulated; i.e., only the probabilities P_4 and P_{-4} are used. If the random number $\xi \leq P_4$, then Θ_{Buf} increases by ΔS ; otherwise Θ_{Buf} decreases by ΔS . After each event, at first the time is increased by $\Delta t = -(\tau_s \ln \xi)/N$ and then the values τ_s , P_4 , and P_{-4} are recalculated in accordance with formulas (3a). The simulation continued until Θ_{Buf} changes by $\Delta\Theta_{\text{Buf}}$ in accordance with the chosen step S_r . Remember that $S_r = \Delta\Theta_s/\Theta_s \ll 1$. After this a pass to the fast subsystem is carried out.

2. Here the molecular events are chosen

by a random number ξ in accordance with probabilities P_1 , P_{-1} , and P_2 .

(i) If adsorption of A occurs and simultaneously $\Theta_B = 0$, then Θ_A increases by ΔS . Otherwise (at $\Theta_B \neq 0$) the value Θ_A does not change and Θ_B decreases by ΔS .

(ii) If adsorption of B_2 occurs, the following situations are analyzed for each of two particles B . (a) If $\Theta_A = 0$, the particle B adsorbs; i.e., Θ_B increases by ΔS . (b) If $\Theta_A \neq 0$, then Θ_B does not change and Θ_A decreases by ΔS .

(iii) If desorption of A occurs then Θ_A decreases by ΔS .

After each event the probabilities P_1 , P_{-1} , P_2 are recalculated by the formulas (3b). The simulation continues until steady state is reached. After this, item 1 is carried out.

In simulating adsorption of A and B_2 particles and the reaction between A and B on the surface, the above sequence of steps (item 2) corresponds with the situation of homogeneous coverage at $K_3 \rightarrow \infty$. As shown (20), in this case the homogeneous coverage of the surface always consists of particles of one kind only, viz. either A or B .

The TSM algorithm has two heuristic parameters, the values of which are to be found experimentally: S_t , a step of change of the slow subsystem; and NM , a number of MC steps required for the fast subsystem to reach a quasi-equilibrium state.

We studied dynamic behavior of the MC model for various values of S_t , from 0.01 to 0.05, and for various values of NM , from 50 to 200. It has been found that $NM = 100$ is sufficient for all values of S_t and further increase of NM did not result in any change of the values measured. We also found that the most suitable value of S_t is 0.02 (as a reasonable compromise between accuracy of results and computational time). In the MC experiment, the initial coverage for buffer particles was $\Theta(0)_{\text{Buf}} = 0.6$ and in the numerical integration, it was $\Theta(0)_{\text{Buf}} = 0$. The numerical integration was performed within the accuracy of $5 \cdot 10^{-4}$. In both cases the same parameter values were used (20).

The rate constant in numerical integration was $K_3 = 1 \cdot 10^4$. Figures 1 and 2 show data of numerical integration and of MC modeling at $S_t = 0.02$, respectively. One can see that the main features, viz. the time scale and the oscillation frequency and amplitudes of Θ_B and Θ_{Buf} coverages, coincide with good accuracy, as do the phase diagrams. The angle-shaped forms in Figs. 2b and 2c and the instability of the oscillation periods in Fig. 2a result from the stepped change of the value, Θ_{Buf} , in the MC experiment. Actually, because of the stepped change, the critical value of Θ_{Buf} (critical point) is defined within the accuracy of $\Delta\Theta_{\text{Buf}} = 0.02\Theta_{\text{Buf}}$. Could we obtain exactly the same dynamics in the MC simulation as in the numerical solution? This estimation has been made for the given values of parameters, and we have found that the indefiniteness of the value of Θ_{Buf} at the critical point can result in the difference between the periods of some oscillations of up to 100 sec. Comparing the curves in Fig. 1a with those in Fig. 2a, one can see that the difference for all periods, except the last one, is about 60 sec. The above data (Figs. 1 and 2) show validity of the TSM algorithm.

THE CASE OF INHOMOGENEOUS SURFACE COVERAGE

In the previous section, to verify the TSM algorithm we used it in the case for which the numerical solution gave correct results. In this section the TSM algorithm is applied to investigate the situation in which the MFA model of mechanism (1) fails completely. We studied the dynamics of mechanism (1) under an inhomogeneous surface coverage. For this purpose we inserted the TSM algorithm into the ordinary scheme of MC simulation described in (11). The results obtained are briefly described below.

For simulation of the surface a square lattice of 40×40 with periodic boundary conditions has been used, the step for the slow processes was $S_t = 0.02$, and the number of MCS for fast processes per one S_t was $NM = 100 - 400$. For plotting time depen-

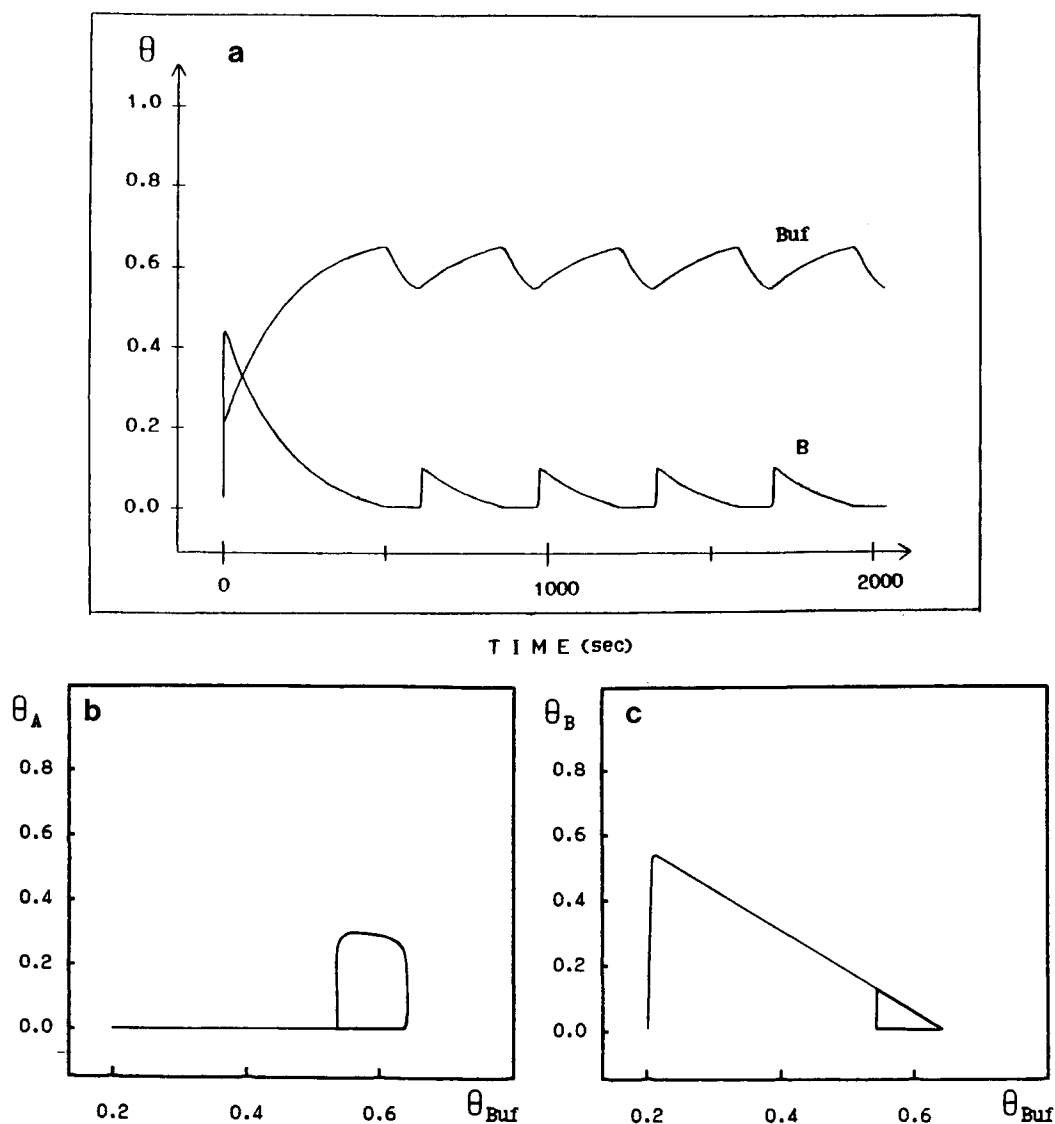


FIG. 1. Numerical integration. Plots of coverages θ_B and θ_{Buf} vs time (a), trajectories on $\theta_A - \theta_{Buf}$ plane (b), trajectories on $\theta_B - \theta_{Buf}$ plane (c). Parameters: $K_1 = 0.85$, $K_{-1} = 0.3$, $K_2 = 1.23$, $K_{-2} = 0$, $K_4 = 0.001$, $K_{-4} = 0.0005$, $K_3 = 10^4$, $\theta(0)_{Buf} = 0$.

dences of the reaction rate we depicted, for convenience, values of reaction rate for every 20 MCS. Magnitudes of the constants of adsorption/desorption of the buffer particles K_4 and K_{-4} are of no importance, as is mentioned above. Only their ratio is essential. In our experiments, $K_4/K_{-4} = 2$. But since the total system changes in the time scale of the slow subsystem, we assign somewhat

arbitrary values of $K_4 = 0.02$ and $K_{-4} = 0.01$ and plot the time dependences directly in seconds.

The region of existence of oscillations runs over, roughly, from $K_1/K_2 \sim 0.7$ up to $K_1/K_2 \sim 1$. In Fig. 3 peak relaxation oscillations at $K_1/K_2 = 1$ are shown. In this case (large partial pressure of A) the system spends most of the time in the state with a

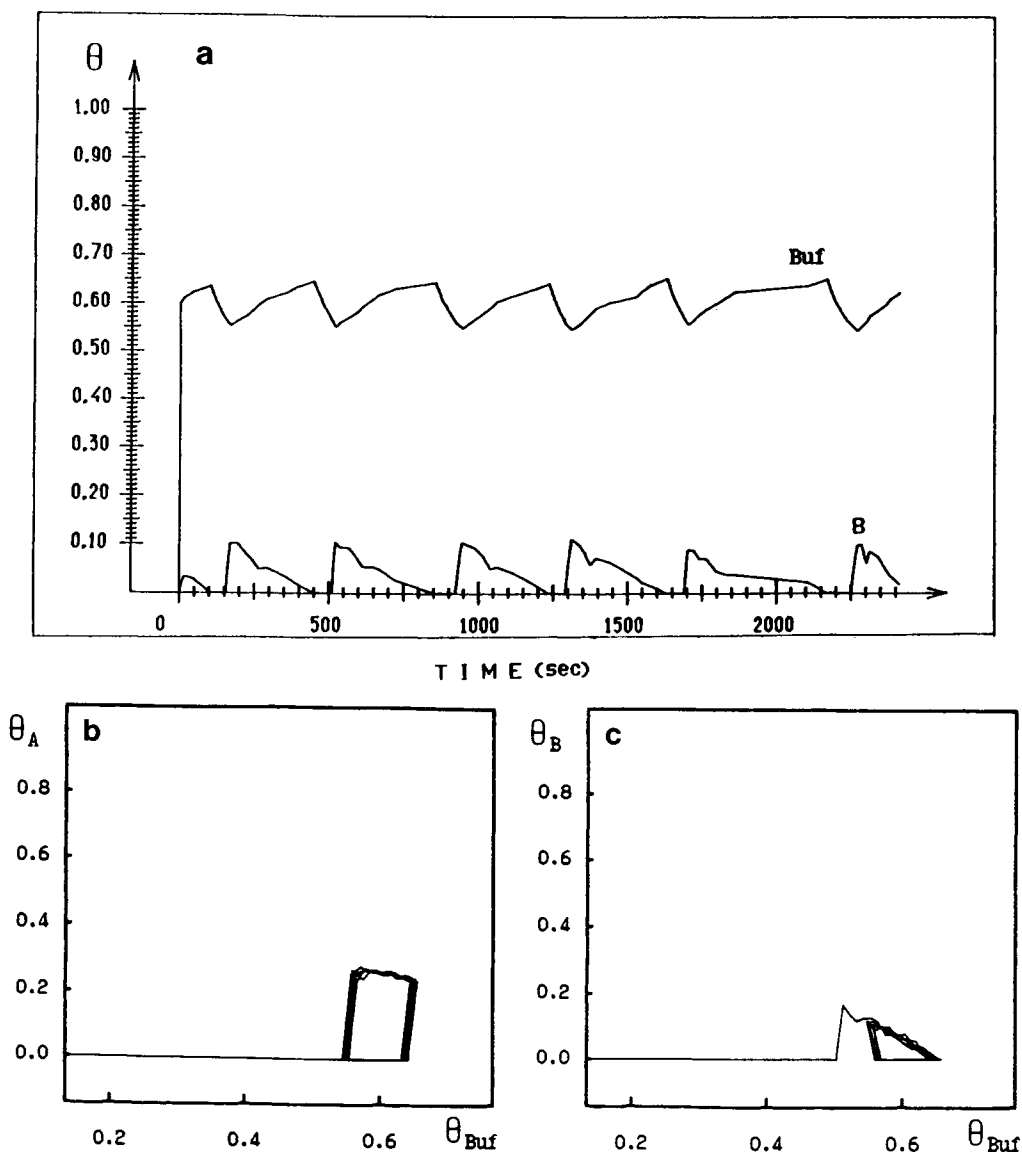


FIG. 2. Monte Carlo simulation. Plots of coverages θ_B and θ_{Buf} vs time (a), trajectories on $\theta_A - \theta_{Buf}$ plane (b), trajectories on $\theta_B - \theta_{Buf}$ plane (c). $K_3 \rightarrow \infty$ $\theta(0)_{Buf} = 0.6$; the remaining parameters are the same as those in Fig. 1.

low reactivity ($\theta_B = 0$, high coverage θ_A) and only a bit of time in the state with high reactivity ($\theta_B \neq 0$, $\theta_A = 0$). As K_1 decreases, the system spends more and more time in the state with high reactivity (Figs. 4 and 5), and oscillations gradually change from sharp peaks to "shelves."

Figures 4 and 6–8 show how the behavior

of the system changes depending on the value of the rate constant of desorption of particle A, i.e., K_{-1} . This constant is a crucial parameter defining the dynamic behavior of the system. As K_{-1} increases, the system passes through an entire sequence of states. At first, at $K_{-1} = 0$, the system is in a nonreactive state. This state is not

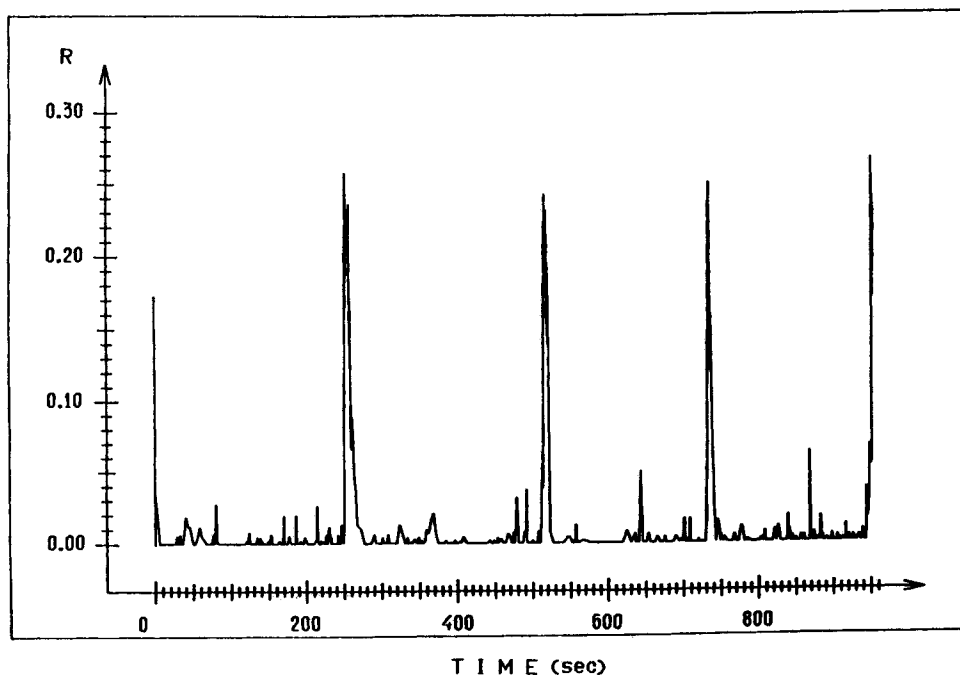


FIG. 3. Plot of reaction rate R vs time. $K_1 = 1$, $K_{-1} = 0.04$, $K_2 = 1$, $K_{-2} = 0$, $K_4 = 0.02$, $K_{-4} = 0.01$, $K_3 \rightarrow \infty$, $\Theta(0)_{\text{Buf}} = 0.15$.

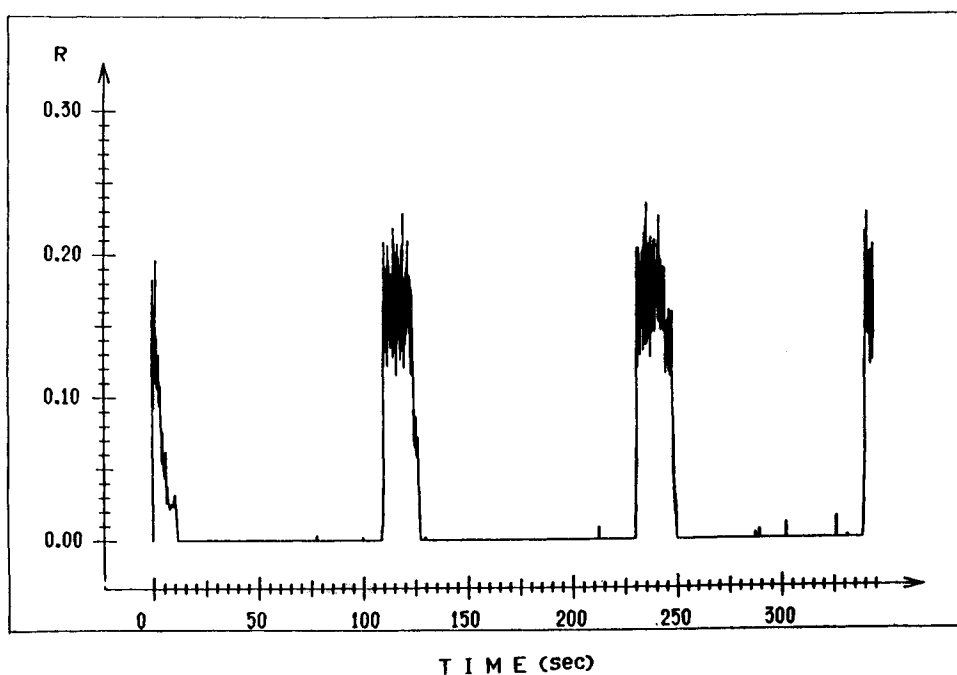


FIG. 4. Plot of reaction rate R vs time. $K_1 = 0.9$; the remaining parameters are the same as those in Fig. 3.

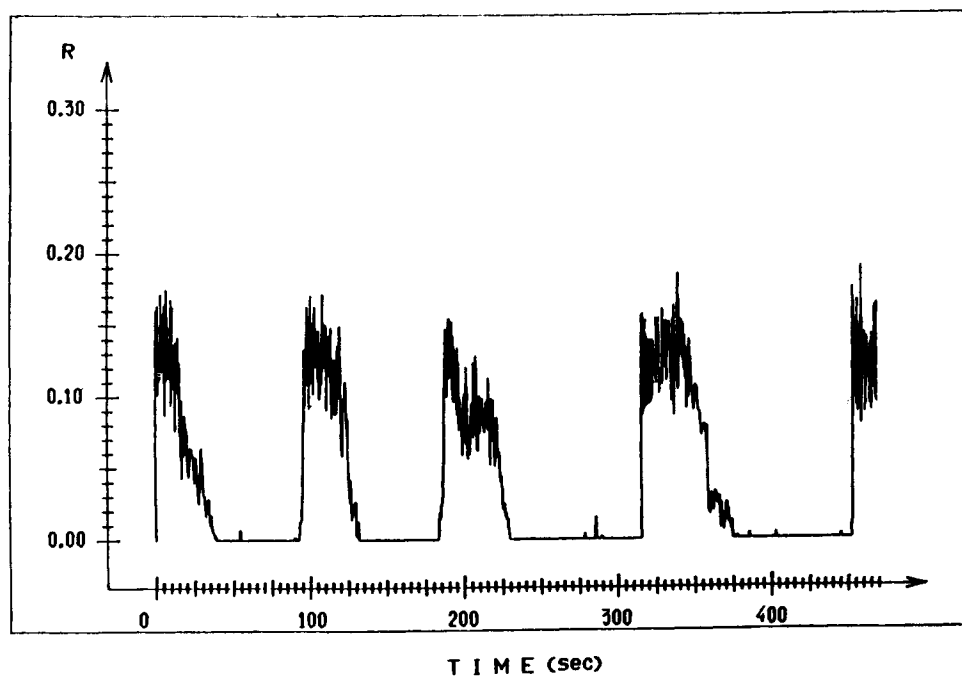


FIG. 5. Plot of reaction rate R vs time. $K_1 = 0.8$; the remaining parameters are the same as those in Fig. 3.

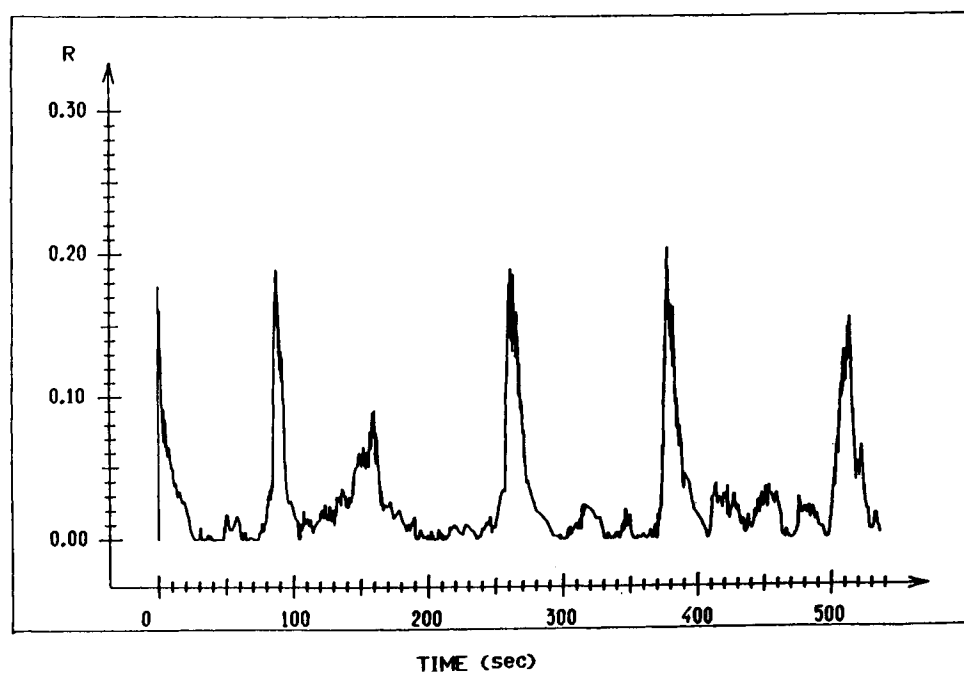


FIG. 6. Plot of reaction rate R vs time. $K_1 = 0.9$, $K_{-1} = 0.016$; the remaining parameters are the same as those in Fig. 3.

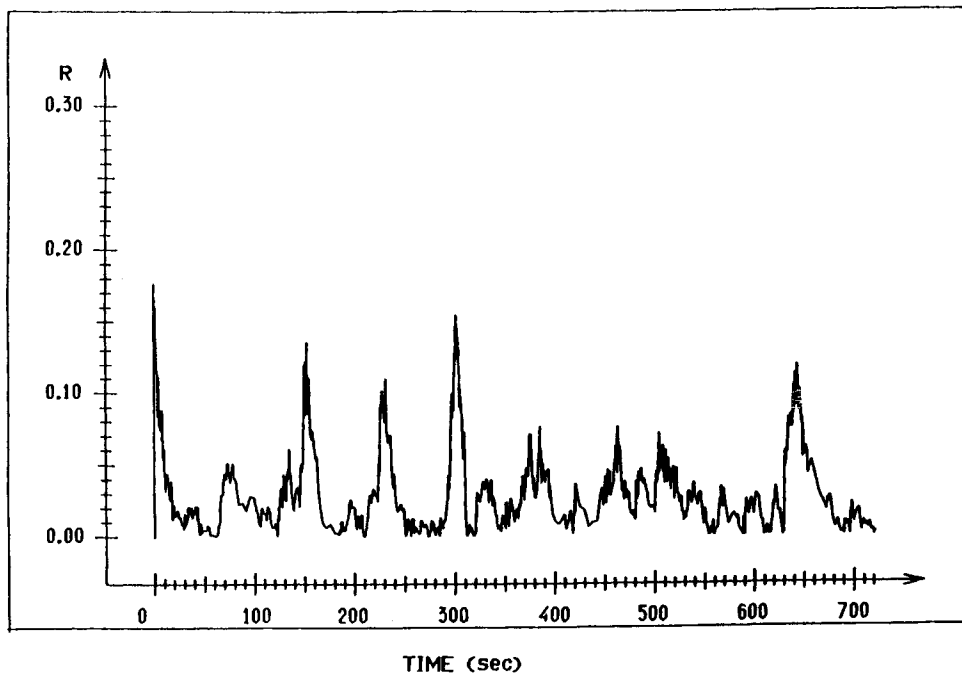


FIG. 7. Plot of reaction rate R vs time. $K_1 = 0.9$, $K_{-1} = 0.024$; the remaining parameters are the same as those in Fig. 3.

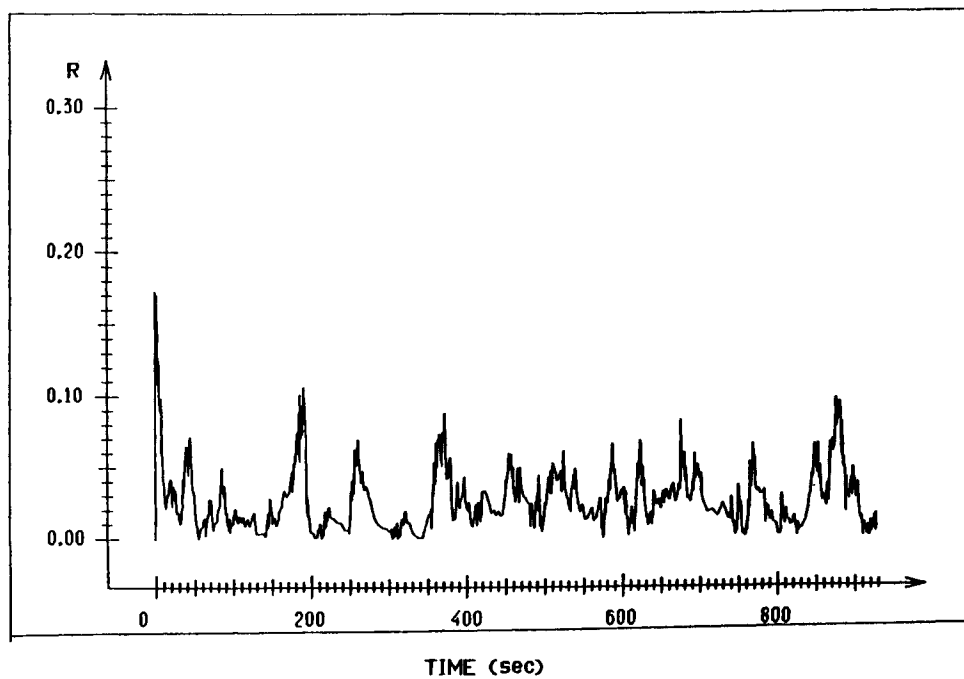


FIG. 8. Plot of reaction rate R vs time. $K_1 = 0.9$, $K_{-1} = 0.028$; the remaining parameters are the same as those in Fig. 3.

shown here. The system then passes into a state with peak relaxation oscillations (Fig. 4) and then into states with more and more chaotic oscillations (Figs. 6–8). At last a nonoscillatory state with a non-zero reaction rate occurs, which is not shown here. Such behavior of the system can be explained reasonably. For convenience, let us designate the high reactivity state ($\Theta_B \neq 0$, $\Theta_A = 0$) as 1 and the low reactivity state ($\Theta_B = 0$, $\Theta_A \neq 0$) as 2. It is evident that as K_{-1} increases, reactivity of state 1 decreases (fewer particles of *A* react), and reactivity of state 2 increases because more empty sites become available for B_2 adsorption. Consequently the difference between the two states decreases, leading to a decrease in the amplitude of oscillations of the reaction rate. Moreover, since values of K_{-1} are large, *A* molecules do not form a compact coverage in state 2, and so the system passes easily from state 2 into state 1 due to small fluctuations in the adsorption of reactants. Thus, the behavior of the system becomes more and more chaotic as K_{-1} increases. A similar behavior in the MC model of reaction $A + B \rightarrow AB$ has been observed (21) on small lattices.

The examples given here demonstrate that the TSM algorithm may be used efficiently to study dynamic behavior of complex chemical systems in which the rates of various processes are considerably different.

CONCLUSION

The algorithm presented attempts to simulate catalytic reactions by MC techniques when there are processes occurring on vastly different time scales. The basic idea is that the correct behavior of stiff systems can be obtained if the system is divided into two subsystems (one consisting of the slow variables and another consisting of the fast ones), which are then simulated separately, each in its own time scale. The fast subsystem is assumed to always be in a quasi-equilibrium state during all changes of the slow subsystem. Then, if the relaxation time

of the fast subsystem is much less than the characteristic time of the slow subsystem, one can use, during MC simulation, much fewer fast events per slow event than the actual physical ratio.

There is some analogy between the suggested approach and the MC simulation methodology of kinetics of thermal desorption processes. In real systems, the activation energy for surface diffusion is known to be about 15–20% of that for desorption, and the ratio of diffusion events per desorption event is very large. Since the ratio is large, the adsorbed overlayer is assumed to be in equilibrium state. MC simulation of thermal desorption is usually conducted as follows: after removing each particle from adlayer (slow event), a new equilibrium among the rest is reached through surface diffusion (fast events). In this case it turns out that equilibrium in the adlayer can be maintained with a much lower ratio of fast events per slow event than the actual physical ratio. Of course, in complex reaction systems the equilibrium state is reached in a more complex way than that in an adlayer of nonreactive particles in the case of nonassociative desorption. But the general criterion is the same in both cases: the relaxation time of the fast subsystem should be much less than the characteristic time of the slow subsystem.

To obtain correct results with the TSM algorithm, two parameters should be found experimentally: S_i and NM. The value of S_i defines the accuracy of the results obtained and the computational time. For the total system not to deviate much from steady state, S_i should be small enough in any case. The effect of such deviation for a complex system may be unexpected. To find the appropriate value of NM it is necessary to take into account that in critical points, the relaxation rate may become very slow (critical slowing-down). In this case, it is convenient to find two values of NM, one near the critical point and one far from it, and use both in a numerical experiment. In order to avoid the influence of the relaxation regime, measurements must be performed after the

fast subsystem reaches equilibrium state. The efficiency of the TSM algorithm increases as the stiffness of the system increases because, as noted above, a computational time does not depend on real time scale of the slow subsystem.

In conclusion, the TSM algorithm was utilized to study the dynamic behavior of the MC model of the heterogeneous catalytic reaction, $A + \frac{1}{2}B \rightarrow AB$, through the Langmuir-Hinshelwood mechanism, supplemented with a slow stage of reversible adsorption of inert particles. The validity of the TSM algorithm was checked through comparison with a numerical solution when we simulated a spatially homogeneous surface coverage. Then the TSM algorithm was used to study the situation in which surface coverage is spatially inhomogeneous and when the numerical method fails. It has been found that, in this case, there exist various relaxation oscillations in the MC model and the desorption rate constant of particles A is a crucial parameter in the formation of oscillations. The TSM algorithm has demonstrated efficiency in resolving problems when analytical/numerical methodology fails and when the traditional scheme of MC simulation requires a very long computational time.

REFERENCES

1. Sheintuch, M., and Schmitz, R. A., *Catal. Rev. Sci. Eng.* **15**, 107 (1977).
2. Jensen, K. F., and Ray, W. H., *Chem. Eng. Sci.* **35**, 241 (1980).
3. Razon, L. F., and Schmitz, R. A., *Catal. Rev. Sci. Eng.* **28**, 89 (1986).
4. Chang, H.-C., and Aluko, M., *Chem. Eng. Sci.* **36**, 1611 (1981).
5. Eigenberger, G., *Chem. Eng. Sci.* **33**, 1263 (1978).
6. Lynch, D. T., and Wanke, S. E., *Can. J. Chem. Eng.* **59**, 766 (1981).
7. Lazman, M. Z., Marshneva, V. I., and Yablonskii, G. S., in "Unsteady State Processes in Catalysis" (Yu. Sh. Matros, Ed.), p. 375. VSP-111, Utrecht, 1990.
8. Suhl, H., *Surf. Sci.* **107**, 88 (1982).
9. Vlachos, D. G., Schmidt, L. D., and Aris, R., University of Minnesota Supercomputer Institute Research Report UMSI 90/104, 1980.
10. Goldshtein, V. M., Sobolev, V. A., and Yablonskii, G. S., *Chem. Eng. Sci.* **41**, 2761 (1986).
11. Ziff, R. M., Gulari, E., and Barshad, Y., *Phys. Rev. Lett.* **56**, 2553 (1986).
12. Sadig, A., *Z. Phys. B: Condens. Matter* **67**, 211 (1987).
13. Meakin, P., and Scalapino, D. J., *J. Chem. Phys.* **87**, 731 (1987).
14. Dumont, M., Poriaux, M., and Dagonnier, R., *Surf. Sci.* **169**, L307 (1986).
15. Araya, P., Porod, W., Sant, R., and Wolf, E. E., *Surf. Sci.* **208**, L80 (1989).
16. Ehsasi, M., Matloch, M., Frank, O., Block, J. H., Christmann, K., Rys, F. S., and Hirschwald, W., *J. Chem. Phys.* **91**, 4949 (1989).
17. Kaukonen, H.-P., and Nieminen, R. M., *J. Chem. Phys.* **91**, 4380 (1989).
18. Fischer, P., and Titulaer, U. M., *Surf. Sci.* **221**, 409 (1989).
19. Bykov, V. I., and Yablonskii, G. S., *React. Kinet. Catal. Lett.* **16**, 377 (1981).
20. Lazman, M. Z., Ph.D. dissertation, Institute of Catalysis, Novosibirsk, 1986.
21. Fichthorn, K., Gulari, E., and Ziff, R., *Chem. Eng. Sci.* **44**, 1403 (1989).